O-458

J. Chem. Thermodynamics **1992,** 24, 661–672

Thermodynamics of ammonium halogenated tellurides

II. Heat capacity, phase transitions, and thermodynamic properties of $(ND_4)_2TeCl_6$ at temperatures from 5 K to 325 K

JANE E. CALLANAN,

Callanan Associates, 2888 Bluff, Suite 429, Boulder, CO 80301, U.S.A.

RON D. WEIR,[a]

Department of Chemistry and Chemical Engineering, Royal Military College of Canada, Kingston, Ontario K7K 5L0, Canada

and EDGAR F. WESTRUM, JR.

Department of Chemistry, University of Michigan, Ann Arbor, MI 48109-1055, U.S.A.

(Received 29 August 1991; in final form 30 October 1991)

The heat capacity of deuterated ammonium hexachlorotellurate $(ND_4)_2TeCl_6$ was measured at temperatures T from 5 K to 325 K by adiabatic calorimetry. A small anomaly in the curve of heat capacity against temperature was found at $T = (89.5 \pm 0.3)$ K with a maximum $C_{p,m} = 23.84 \cdot R$, $\Delta_{trs}S^\circ_m = (0.234 \pm 0.006) \cdot R$. The discovery of this anomaly supports the presence of a rotative displacive transition similar to that involving $TeCl_6^{2-}$ in the undeuterated salt. In addition, two λ-shaped transitions were discovered at $T = (31.4 \pm 0.1)$ K, with a maximum $C_{p,m} = 34.7 \cdot R$, $\Delta_{trs}S^\circ_m = (0.861 \pm 0.007)\,R$, and at $T = (47.6 \pm 0.1)$ K, with a maximum $C_{p,m} = 18.6\,R$, $\Delta_{trs}S^\circ_m = (0.247 \pm 0.006)\,R$. Smoothed values of the standard thermodynamic quantities for pure $(ND_4)_2TeCl_6$ are tabulated up to $T = 320$ K.

1. Introduction

The ammonium hexahalogenated metal salts in the family $(NH_4)_2MX_6$ (M, a transition metal or polyvalent ion; and X, a halogen) usually crystallize at room temperature into a cubic antifluorite structure of space group Fm3m or No. 225 O_h^5 and are ideal models for studying molecular motion in solids. The NH_4^+ ion, situated at a tetrahedral lattice site, is able to overcome the low barrier to rotation about its

[a] To whom correspondence should be sent.

0021–9614/92/060661 + 12 $02.00/0

threefold axis. At room temperature, NH_4^+ experiences classical hindered rotation and, at temperatures $T < 40$ K, quantum-mechanical tunnelling. Some salts in this family undergo structural phase transitions and change into a phase of lower symmetry as the temperature is lowered.[1] Other salt pairs, *e.g.* K_2SnCl_6,[2] and $(NH_4)_2SnCl_6$;[2] and K_2OsCl_6,[3,4] and $(NH_4)_2OsCl_6$,[5] show no evidence of a transition in spite of its presence in the alkali analogue. The $(NH_4)_2PtCl_6$,[6] and $(ND_4)_2PtCl_6$,[7] pair is an example where a structural transition occurs in the deuterated analogue which is absent from the ammoniated salt.

The pair $(NH_4)_2TeCl_6$ and $(ND_4)_2TeCl_6$ is particularly interesting in that experimental results of ^{35}Cl n.q.r. and Raman spectra at low temperatures suggest a structural phase transition near $T = 85$ K in both compounds.[8-11] That the deuteration failed to affect this transition indicates that the anomaly is probably not associated with rotational motion of the NH_4^+. Neutron-diffraction studies confirmed the transition at $T = 85$ K in $(NH_4)_2TeCl_6$ and showed that the high-temperature cubic Fm3m structure changes to trigonal $\bar{R}3$ at $T < 85$ K. This transition is classified as rotative displacive in which the static rotation angle of the $TeCl_6^{2-}$ octahedral ion shifts by a few times $\pi/180$ relative to its orientation in the cubic phase. In addition, a small distortion of the lattice and a slight displacement of the NH_4^+ occur along the 111 direction. Recent adiabatic-calorimetric experiments on $(NH_4)_2TeCl_6$ revealed a continuous curve of heat capacity against temperature from $T = 5$ K to $T = 350$ K, but with a small anomaly near $T = 86$ K for which the transitional entropy increment $\Delta_{68\,K}^{98\,K} S_{trs}^{\circ}$ amounted to only $(0.071 \pm 0.028) \cdot R = R \cdot \ln 1.07$.[12] This finding is consistent with the subtle change of the rotative displacive transition.

Whereas $(NH_4)_2TeCl_6$ shows no further transitions at lower temperatures, such is not the case for $(ND_4)_2TeCl_6$. Results from ^2D n.m.r., ^{35}Cl n.q.r., and Raman spectroscopy suggest additional transitions at $T = 45$ K and $T = 25$ K involving the cations.[8,11] However, no crystallographic studies have yet been reported on the structures involved. In this paper, we report adiabatic heat-capacity measurements on $(ND_4)_2TeCl_6$, which were undertaken to determine the enthalpy and entropy of the transitions.

2. Experimental

The sample of $(ND_4)_2TeCl_6$ was provided by Professor J. Pelzl of Ruhr Universität, Bochum, Federal Republic of Germany. The Guinier–de-Wolff diffraction pattern done on the $(ND_4)_2TeCl_6$ sample when received by us was in agreement with the standard pattern for this compound and $(NH_4)_2TeCl_6$: No. 9-392 as determined by the Joint Committee for Powder Diffraction Standards.[13-15] Its structure was face-centred cubic at room temperature with $a = (1.0200 \pm 0.0002)$ nm, which compares with $a = (1.0194 \pm 0.0002)$ nm for $(NH_4)_2TeCl_6$.[12]

The molar heat capacity $C_{p,m}$ was measured from $T = 5$ K to $T = 325$ K by adiabatic calorimetry in the Mark XIII adiabatic cryostat, which is an upgraded version of the Mark II cryostat described previously.[16] A guard shield was incorporated to surround the adiabatic shield. A Leeds and Northrup capsule-type

platinum resistance thermometer (laboratory designation A-5) was used for temperature measurements. The thermometer was calibrated at the U.S. National Bureau of Standards (N.B.S., now NIST) against the IPTS-1948 (as revised in 1960)[17] for temperatures above 90 K, against the N.B.S. (NIST) provisional scale from 10 K to 90 K, and by the technique of McCrackin and Chang[18] below 10 K. These calibrations are estimated to reproduce thermodynamic temperatures to within 0.03 K between 10 K and 90 K and within 0.04 K above 90 K.[19] The effects of changing the temperature scale to ITS-90 vary over the range $90 \leqslant T/\mathrm{K} \leqslant 350$ from $+0.020 \leqslant (T_{90} - T_{48})/\mathrm{K} \leqslant -0.27$, and for the range $14 \leqslant T/\mathrm{K} \leqslant 90$ from $-0.008 \leqslant (T_{90} - T_{55})/\mathrm{K} \leqslant 0.018$.[21,22] The changes in heat capacity, enthalpy, and entropy resulting from the conversion from IPTS-68 to ITS-90 have been shown for a number of materials to lie within the experimental error of the measurements over the range from $T = 16$ K to $T = 2800$ K.[20] Measurements of mass, current, potential difference, and time were based upon calibrations done at N.B.S. (NIST). The heat capacities from about $T = 5$ K to $T = 350$ K were acquired with the assistance of a computer, which was programmed for a series of determinations.[22,23] During the drift periods, both the calorimeter temperature and its first and second derivatives of temperature with respect to time were recorded to establish the equilibrium temperature of the calorimeter before and after the energy input. While the calorimeter was operating, the heater current and potential difference as well as the duration of the heating interval were determined. Also recorded was the apparent heat capacity of the system, which included the calorimeter, heater, thermometer, and sample.

A gold-plated copper calorimeter (laboratory designation W-99) with four internal vertical vanes and a central entrant well for (heater + thermometer) was loaded with $(ND_4)_2TeCl_6$. After loading, the calorimeter was evacuated and pumping was continued for several hours to ensure that moisture was no longer present in the sample. After addition of about $p = 30$ kPa (at $T = 300$ K) of helium gas to the vessel to facilitate thermal equilibration, it was then sealed by means of an annealed gold gasket tightly pressed on to the stainless-steel knife edge of the calorimeter top with a screw closure about 5 mm in diameter.

Buoyancy corrections were calculated on the basis of a crystallographic density of $2.406\ \mathrm{g \cdot cm^{-3}}$ derived from the unit-cell edge of our sample. The mass of the $(ND_4)_2TeCl_6$ was 6.77675 g ($\triangleq 0.0176275$ mol based on its molar mass of $384.442\ \mathrm{g \cdot mol^{-1}}$ calculated from the 1985 IUPAC recommended relative atomic masses of the elements).[24]

The thermal history of the $(ND_4)_2TeCl_6$ is represented by the following linear array. The arrows denote either cooling or heating, which correspond to the acquisition of heat-capacity results.

$$300\ \mathrm{K} \xrightarrow{33\ \mathrm{h}} 5\ \mathrm{K} \underset{\text{Series I}}{\xrightarrow{7\ \mathrm{h}}} 42\ \mathrm{K} \xrightarrow{3\ \mathrm{h}} 22\ \mathrm{K} \underset{\text{Series II}}{\xrightarrow{6\ \mathrm{h}}} 56\ \mathrm{K}$$

$$\xrightarrow{2\ \mathrm{h}} 45\ \mathrm{K} \underset{\text{Series III}}{\xrightarrow{24\ \mathrm{h}}} 325\ \mathrm{K}.$$

3. Results

The experimental molar heat capacities for $(ND_4)_2TeCl_6$ are presented in table 1, where the temperature T represents the midpoint of the temperature intervals. The measurements were made in three series beginning at $T = 5.2$ K and ending at $T = 325$ K. Except for experimental points in the region of the λ-shaped anomaly, the standard errors in our heat-capacity values vary from $\approx 0.01 \cdot C_{p,m}$ at $T = 10$ K to $< 0.005 \cdot C_{p,m}$ at $T > 25$ K. The heat capacity of the sample represented about 0.40 to 0.80 of the measured total heat capacity away from the regions of the anomalies.

The sample was supplied as a fine yellow powder and judged not to require further grinding. Particle size and thermal history are factors that influence hysteresis effects in some ammonium compounds.[25-27] Once loaded into the calorimeter, our sample of $(ND_4)_2TeCl_6$ was cooled directly from 300 K to 5 K in 33 h, when the measurements began. No differences are apparent among the heat-capacity values in the region of overlap from our three series of measurements.

A plot of experimental values of $C_{p,m}/T$ against T from $T = 6.6$ K to $T = 322$ K is shown in figure 1, where three anomalies are evident. One λ-shaped transition peaks with very high values around $T = 31$ K, and two smaller anomalies reach their maxima near $T = 47$ K and $T = 90$ K. By carrying out heat-capacity measurements with sufficiently small temperature intervals, the temperature where the heat capacity of each reaches its peak was found to be $T = (31.4 \pm 0.1)$ K, $T = (47.6 \pm 0.1)$ K, and

TABLE 1. Experimental molar heat capacity of $(ND_4)_2TeCl_6$
($M = 384.442$ g·mol^{-1}; $R = 8.31451$ J·K^{-1}·mol^{-1})

T/K	$C_{p,m}/R$	T/K	$C_{p,m}/R$	T/K	$C_{p,m}/R$	T/K	$C_{p,m}/R$	T/K	$C_{p,m}/R$
Series I		Series II		47.28	16.95	97.76	23.97	197.09	31.47
6.59	0.148	23.74	4.317	47.89	16.92	99.54	24.21	202.33	31.72
8.24	0.339	25.49	4.943	48.60	14.94	101.35	24.38	207.53	31.96
9.00	0.462	27.37	5.699	49.33	15.09	103.27	24.65	212.71	32.13
10.05	0.613	29.28	6.842	50.04	15.22	105.49	24.90	217.89	32.30
11.24	0.809	30.67	13.43	51.00	15.13	108.11	25.30	223.10	32.47
12.52	1.083	31.41	34.74	52.97	15.74	110.98	25.66	228.31	32.61
13.86	1.387	32.09	15.97	55.78	16.73	114.13	25.98	233.63	32.83
15.21	1.741	33.16	9.522	58.75	17.37	117.69	26.33	239.07	33.01
16.62	2.092	34.37	9.976	61.72	18.33	121.73	26.70	244.48	33.18
18.05	2.491	35.52	10.55	64.68	18.88	126.02	27.17	249.89	33.33
19.58	2.947	36.59	10.88	67.82	19.58	130.61	27.62	255.44	33.46
21.21	3.477	37.77	11.38	71.12	20.30	135.43	28.01	261.18	33.67
22.87	4.006	39.31	12.07	74.60	21.22	140.12	28.40	266.89	33.82
24.54	4.639	41.30	12.76	78.66	22.11	144.87	28.68	272.53	33.98
26.23	5.241	43.15	13.46	81.64	22.67	149.62	28.90	278.18	34.19
27.93	6.017	44.62	14.18	83.31	22.94	154.51	29.29	283.75	34.36
29.67	7.559	46.23	15.38	85.20	23.33	159.70	29.59	289.36	34.53
31.00	23.26	48.04	15.82	87.06	23.73	165.10	29.83	294.89	34.67
32.92	12.77	50.26	15.05	88.90	23.84	170.50	30.17	300.39	34.82
35.94	10.61	52.73	15.64	90.73	23.82	175.87	30.57	305.86	34.95
38.84	11.85	55.05	16.47	92.51	23.50	181.20	30.81	311.31	35.11
41.40	12.91	Series III		94.29	23.49	186.56	31.02	316.75	35.25
		45.40	14.45	96.03	23.70	191.83	31.26	322.17	35.42

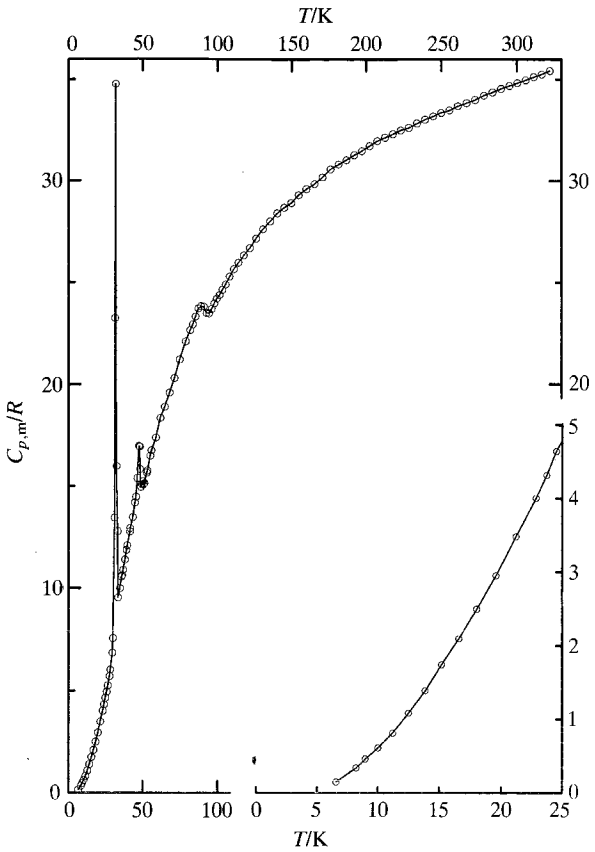

FIGURE 1. Experimental molar heat capacities $C_{p,m}$ at constant pressure plotted against temperature T for $(ND_4)_2TeCl_6$. The region $T < 25$ K is enlarged in the lower right-hand corner.

$T = (89.5 \pm 0.3)$ K for these three anomalies. Two passes were made through the region of the λ-shaped transition at 31 K (see the thermal history above, Series I and II) and reproducible heat capacities resulted. The details of this peak and of that at $T = 47$ K are shown in figure 2. The point at $T = 32.92$ K with $C_{p,m}/R = 12.77$ contains a contribution from the λ-shaped transition at $T = 31$ K causing it to lie off the smooth curve. The reproducibility of our measurements of the enthalpy and entropy changes through these regions is indicated in tables 2 and 3 where the transition enthalpy and entropy increments are listed.

The anomaly centred about $T = 90$ K is shown in detail in figure 3, where the continuous curve reaches its greatest divergence from the lattice curve at $T = 89.5$ K and merges again with the lattice heat capacity at $T = 95$ K. The excess molar enthalpy and entropy associated with the anomaly amount respectively to $\Delta_{trs}H^\circ_m = \Delta^{95\,K}_{65\,K}H^\circ_m = (19.22 \pm 0.04) \cdot R \cdot K$ and $\Delta_{trs}S^\circ_m = \Delta^{95\,K}_{65\,K}S^\circ_m = (0.234 \pm 0.006) \cdot R$, where $R = 8.31451\ J \cdot K^{-1} \cdot mol^{-1}$. The reproducibility of our measurements of the enthalpy

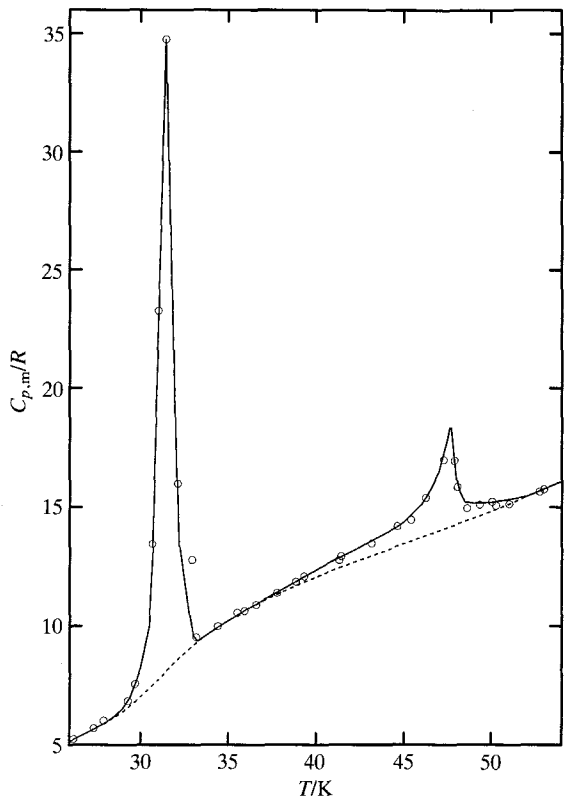

FIGURE 2. Experimental molar heat capacities $C_{p,m}$ at constant pressure plotted against temperature T through the region of the two lowest λ-shaped transitions from about $T = 25$ K to $T = 55$ K for $(ND_4)_2TeCl_6$. – – –, The lattice heat capacity.

TABLE 2. Summary of the thermophysical quantities through the transition at $T_{trs} = (31.4 \pm 0.1)$ K for $(ND_4)_2TeCl_6$ ($R = 8.31451\ J \cdot K^{-1} \cdot mol^{-1}$). T_1 and T_2 denote the beginning and ending temperatures, respectively, for two enthalpy determinations (Series I and II) through the transitions

	T_1/K	T_2/K	$\Delta_{T_1}^{T_2} H_m^\circ/(R \cdot K)$	$\Delta_{28K}^{33.5K} H_m^\circ/(R \cdot K)$	$\Delta_{28K}^{33.5K} S_m^\circ/R$
	27.080	34.394	82.84	68.89[a]	
	28.411	33.789	69.14	68.85[a]	
			Mean:	68.87 ± 0.02	
Graphical integration:				68.89 ± 0.01[b]	2.217 ± 0.004
Lattice contribution:				41.88 ± 0.01[c]	1.356 ± 0.003
$\Delta_{trs} H_m^\circ/(R \cdot K)$:				26.99 ± 0.03	
$\Delta_{trs} S_m^\circ/R$:					0.861 ± 0.007

[a] Independent determinations.

[b] Error due to the uncertainty in the position of the experimental heat-capacity curve through the peak of the transition.

[c] Error due to the uncertainty in the position of the lattice heat-capacity curve through the region of the transition.

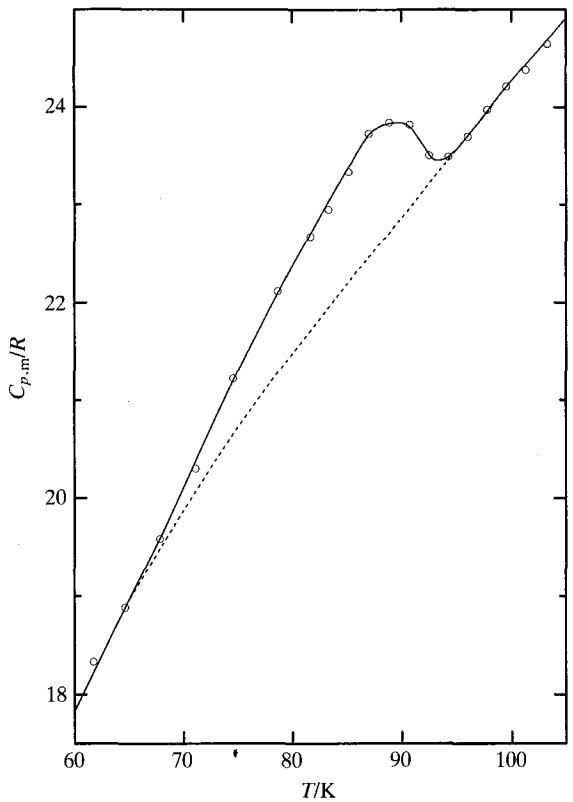

FIGURE 3. Experimental molar heat capacities $C_{p,m}$ at constant pressure plotted against temperature T through the region of the uppermost transition from about $T = 70$ K to $T = 100$ K for $(ND_4)_2TeCl_6$. — — —, The lattice heat capacity.

and entropy changes through this region is indicated in table 4, where the transition enthalpy and entropy increments are listed. Integration of the smoothed heat capacities and the enthalpy and entropy increments through the anomalies yielded the thermodynamic functions. The smoothed curve of heat capacity was made by a spline fit to the experimental points, except in the region of the anomalies where the curve was hand-drawn to yield enthalpies in agreement with those determined experimentally and shown in tables 2 to 4. Values of $C_{p,m}/R$ and the derived functions are presented at selected temperatures in table 5. The corresponding values for the lattice heat capacities beneath the two anomalies, drawn by smooth interpolation of the curves, are shown in parentheses and plotted in figures 2 and 3 as broken lines. The smooth lattice curve touches the solid line from $T = 33.5$ K to $T = 36.5$ K. In assessing the enthalpy and entropy changes associated with these two anomalies, the "extra" heat capacity above $T = 36.5$ K was taken to belong to the upper anomaly in figure 2, and that below $T = 33.5$ K was assigned to the lower-temperature anomaly. The heat capacities of $(ND_4)_2TeCl_6$ below $T = 6$ K were

TABLE 3. Summary of the thermophysical quantities through the transition at $T_{trs} = (47.6 \pm 0.1)$ K for $(ND_4)_2TeCl_6$ ($R = 8.31451\ J \cdot K^{-1} \cdot mol^{-1}$). T_1 and T_2 denote the beginning and ending temperatures, respectively, for enthalpy determinations (Series I and II) through the anomaly

	T_1/K	T_2/K	$\Delta_{T_1}^{T_2} H_m^\circ/(R \cdot K)$	$\Delta_{36.5\,K}^{52\,K} H_m^\circ/(R \cdot K)$	$\Delta_{36.5\,K}^{52\,K} S_m^\circ/R$
Experimental	36.066	151.528	213.79	216.37	
Graphical integration:				216.40 ± 0.02 [a]	4.884 ± 0.004
Lattice contribution:				204.87 ± 0.02 [b]	4.637 ± 0.002
$\Delta_{trs} H_m^\circ/(R \cdot K)$:				11.50 ± 0.04	
$\Delta_{trs} S_m^\circ/R$:					0.247 ± 0.006

[a] Error due to the uncertainty in the position of the experimental heat-capacity curve through the peak of the anomaly.

[b] Error due to the uncertainty in the position of the lattice heat-capacity curve through the region of the anomaly.

TABLE 4. Summary of the thermophysical quantities through the transition at $T_{trs} = (89.5 \pm 0.1)$ K for $(ND_4)_2TeCl_6$ ($R = 8.31451\ J \cdot K^{-1} \cdot mol^{-1}$). T_1 and T_2 denote the beginning and ending temperatures, respectively, for enthalpy determinations (Series III) through the anomaly

	T_1/K	T_2/K	$\Delta_{T_1}^{T_2} H_m^\circ/(R \cdot K)$	$\Delta_{65\,K}^{95\,K} H_m^\circ/(R \cdot K)$	$\Delta_{65\,K}^{95\,K} S_m^\circ/R$
Experimental	63.149	95.174	699.87	661.07	
Graphical integration:				661.06 ± 0.02 [a]	8.229 ± 0.004
Lattice contribution:				641.85 ± 0.02 [b]	8.065 ± 0.002
$\Delta_{trs} H_m^\circ/(R \cdot K)$:				19.22 ± 0.04	
$\Delta_{trs} S_m^\circ/R$:					0.234 ± 0.006

[a] Error due to the uncertainty in the position of the experimental heat-capacity curve through the peak of the anomaly.

[b] Error due to the uncertainty in the position of the lattice heat-capacity curve through the region of the anomaly.

obtained by fitting our experimental values below $T = 20$ K to the limiting form of the Debye equation, with a plot of $C_{p,m}/T^3$ against T^2 and extrapolation to $T \rightarrow 0$; see equation (3).

4. Discussion

The quantity measured calorimetrically is $C_{sat,m}$, the heat capacity of the solid or liquid in equilibrium with its saturated vapour. For solid $(ND_4)_2TeCl_6$, $C_{sat,m}$ is virtually identical with $C_{p,m}$ as the right-hand side of the equation:

$$C_{sat,m} - C_{p,m} = (\partial p/\partial T)_{sat}\{(\partial H_m/\partial p)_T - V_m\}. \quad (1)$$

is negligible. The pressure effect of the helium exchange gas (0.2 kPa of helium at 20 K) on the heat capacity of solid $(ND_4)_2TeCl_6$, *i.e.* $(\partial C_{p,m}/\partial p)_T$, is also negligible. However, analysis of heat-capacity results requires $C_{V,m}$, which is related to $C_{p,m}$:

$$C_{p,m} - C_{V,m} = V_m T \alpha^2/\kappa_T, \quad (2)$$

where $\alpha = V_m^{-1}(\partial V_m/\partial T)_p$ is the isobaric expansivity, V_m is the molar volume, and

TABLE 5. Standard molar thermodynamic functions for $(ND_4)_2TeCl_6$

($M = 384.44168\ g \cdot mol^{-1}$; $p^\circ = 101.325\ kPa$; $R = 8.31451\ J \cdot K^{-1} \cdot mol^{-1}$; $\Phi_m^\circ \overset{def}{=} -\Delta_0^T H_m^\circ/T + \Delta_0^T S_m^\circ$)

$\frac{T}{K}$	$\frac{C_{p,m}}{R}$	$\frac{\Delta_0^T S_m^\circ}{R}$	$\frac{\Delta_0^T H_m^\circ}{R \cdot K}$	$\frac{\Phi_m^\circ}{R}$	$\frac{T}{K}$	$\frac{C_{p,m}}{R}$	$\frac{\Delta_0^T S_m^\circ}{R}$	$\frac{\Delta_0^T H_m^\circ}{R \cdot K}$	$\frac{\Phi_m^\circ}{R}$
0	0	0	0	0	100	24.27	24.11	1376.2	10.35
5	(0.0750)	(0.0252)	(0.0977)	(0.0057)		(24.27)	(22.76)	(1318.4)	(9.576)
10	0.600	0.201	1.52	0.049	110	25.53	26.48	1625.2	11.71
15	1.625	0.621	6.88	0.163		(25.53)	(25.13)	(1567.5)	(10.88)
20	3.100	1.281	18.54	0.354	115	26.09	27.63	1754.3	12.37
25	4.790	2.146	38.11	0.622		(26.09)	(26.28)	(1696.5)	(11.53)
28	5.910	2.750	54.13	0.817	120	26.61	28.75	1886.1	13.03
29	6.540	2.967	60.33	0.887		(26.61)	(27.40)	(1828.3)	(12.17)
	(6.395)[a]	(2.966)	(60.27)	(0.887)	125	27.09	29.85	2020.4	13.68
30	8.220	3.214	67.60	0.960		(27.09)	(28.50)	(1962.6)	(12.80)
	(7.025)	(3.193)	(66.98)	(0.960)	130	27.56	30.92	2157.0	14.33
31	22.60	3.614	79.84	1.038		(27.56)	(29.57)	(2099.2)	(13.42)
	(7.745)	(3.435)	(74.36)	(1.036)	135	27.97	31.97	2295.8	14.96
32	17.60	4.447	106.0	1.133		(27.97)	(30.62)	(2238.1)	(14.04)
	(8.505)	(3.693)	(82.49)	(1.115)	140	28.36	32.99	2436.7	15.58
33	9.600	4.824	118.3	1.240		(28.36)	(31.64)	(2378.9)	(14.65)
	(9.195)	(3.965)	(91.35)	(1.197)	145	28.71	33.99	2579.4	16.20
34	9.735	5.109	127.8	1.350		(28.71)	(32.64)	(2521.6)	(15.25)
	(9.735)	(4.248)	(100.8)	(1.283)	150	29.02	34.97	2723.7	16.81
35	10.22	5.398	137.8	1.461		(29.02)	(33.62)	(2666.0)	(15.85)
	(10.22)	(4.537)	(110.8)	(1.372)	160	29.61	36.86	3016.9	18.01
40	12.35	6.903	194.3	2.046		(29.61)	(35.51)	(2959.2)	(17.02)
	(12.05)	(6.030)	(166.8)	(1.860)	170	30.19	38.67	3315.9	19.17
45	14.36	8.471	260.9	2.673		(30.19)	(37.33)	(3258.2)	(18.16)
	(13.45)	(7.532)	(230.6)	(2.407)	180	30.73	40.42	3620.6	20.30
46	15.11	8.795	275.7	2.802		(30.73)	(39.07)	(3562.9)	(19.28)
	(13.72)	(7.830)	(244.2)	(2.522)	190	31.19	42.09	3930.3	21.40
47	16.44	9.133	291.4	2.933		(31.19)	(40.74)	(3872.5)	(20.36)
	(13.99)	(8.128)	(258.0)	(2.638)	200	31.62	43.70	4244.3	22.48
48	16.20	9.500	308.8	3.066		(31.62)	(42.35)	(4186.6)	(21.42)
	(14.26)	(8.425)	(272.2)	(2.755)	210	32.03	45.25	4562.6	23.53
49	15.17	9.817	324.2	3.201		(32.03)	(43.91)	(4504.9)	(22.46)
	(14.53)	(8.722)	(286.6)	(2.874)	220	32.37	46.75	4884.6	24.55
50	15.21	10.12	339.4	3.336		(32.37)	(45.41)	(4826.9)	(23.46)
	(14.82)	(9.019)	(301.2)	(2.994)	230	32.70	48.20	5210.0	25.55
55	16.40	11.62	417.8	4.021		(32.70)	(46.85)	(5152.2)	(24.45)
	(16.40)	(10.50)	(379.3)	(3.609)	240	33.04	49.60	5538.7	26.52
60	17.83	13.11	503.6	4.717		(33.04)	(48.25)	(5480.9)	(25.41)
	(17.83)	(12.00)	(465.0)	(4.246)	250	33.34	50.95	5870.6	27.47
65	18.95	14.58	595.5	5.419		(33.34)	(49.61)	(5812.8)	(26.35)
	(18.95)	(13.47)	(557.0)	(4.899)	260	33.64	52.27	6205.4	28.40
70	20.10	16.03	693.1	6.125		(33.64)	(50.92)	(6147.7)	(27.27)
	(19.87)	(14.91)	(654.1)	(5.563)	270	33.93	53.54	6543.3	29.31
75	21.29	17.45	796.6	6.833		(33.93)	(52.19)	(6485.5)	(28.17)
	(20.72)	(16.31)	(755.6)	(6.233)	280	34.25	54.78	6884.1	30.19
80	22.37	18.86	905.8	7.541		(34.25)	(53.43)	(6826.4)	(29.05)
	(21.47)	(17.67)	(861.1)	(6.905)	290	34.54	55.99	7228.1	31.06
85	23.35	20.25	1020.1	8.248		(34.54)	(54.64)	(7170.3)	(29.91)
	(22.18)	(18.99)	(970.2)	(7.577)	300	34.82	57.16	7574.9	31.91
87	23.71	20.80	1067.2	8.530		(34.82)	(55.82)	(7517.2)	(30.76)
	(22.45)	(19.51)	(1014.8)	(7.846)	310	35.06	58.31	7923.8	32.75
90	23.84	21.60	1138.6	8.953		(35.06)	(56.96)	(7866.1)	(31.59)
	(22.86)	(20.28)	(1082.8)	(8.248)	320	35.34	59.42	8275.8	33.56
92	23.61	22.13	1186.1	9.234		(35.34)	(58.08)	(8218.1)	(32.40)
	(23.14)	(20.78)	(1128.8)	(8.514)	325	34.48	59.97	8450.4	33.96
95	23.56	22.88	1256.6	9.653		(34.48)	(58.62)	(8392.6)	(32.80)
	(23.56)	(21.53)	(1198.8)	(8.914)	298.15	34.79	56.95	7510.5	31.76
						±0.03	±0.06	±7.4	±0.03

[a] Quantities in parentheses represent the values taken on the lattice curve.

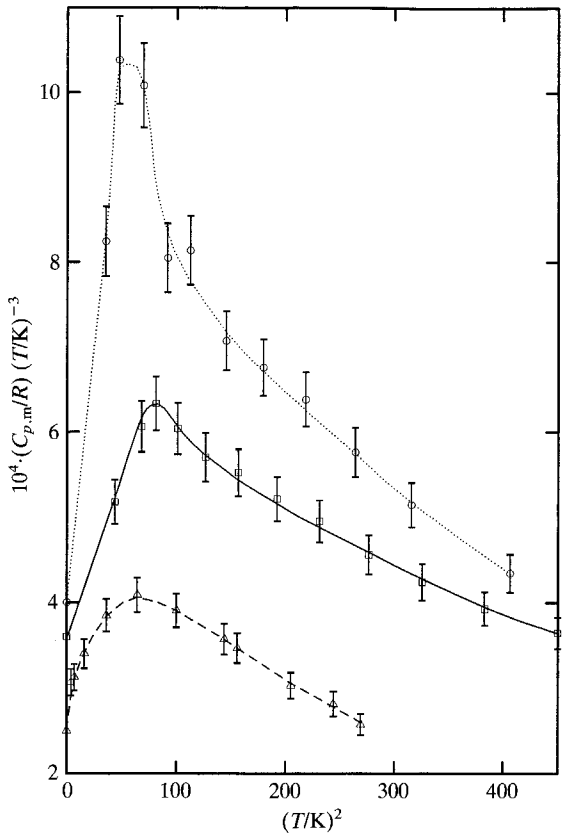

FIGURE 4. Experimental values of $C_{p,m}/RT^3$ plotted against T^2 for $(ND_4)_2TeCl_6$: ——, this work; · · · ·, $(NH_4)_2TeCl_6$ (reference 7); — — —, argon (references 26 and 27). The vertical bars represent about $0.1 \cdot C_{p,m}$.

$\kappa_T = -V_m^{-1}(\partial V_m/\partial p)_T$ is the isothermal compressibility. Values of α and κ_T are unavailable for $(ND_4)_2TeCl_6$ but, fortunately, at $T < 20$ K, $(C_{p,m} - C_{V,m}) \approx 0$.

The heat capacity of an insulator at very low temperatures can be described by a power series of the form:

$$C_{V,m} = aT^3 + bT^5 + cT^7 + \cdots, \tag{3}$$

in which the parameters a, b, and c are directly related to the corresponding power series for the frequency spectrum at low frequencies.[28] As $T \to 0$, the lattice heat capacity of the crystal should become equal to that of an elastic continuum and can be described by the "Debye T^3" law:

$$C_{V,m} = aT^3, \tag{4}$$

$$\Theta_0^C = (12\pi^4 Lk/5a)^{1/3}, \tag{5}$$

where Θ_0^C is the Debye temperature derived from heat capacity and L and k are the Avogadro constant and the Boltzmann constant.

A plot of $C_{p,m}/RT^3$ against T^2 shown in figure 4 is also useful for identifying any non-vibrational contributions to the heat capacity at low temperatures. In the region $36 < (T^2/K^2) < 400$, the graph of our experimental heat capacities for $(ND_4)_2TeCl_6$ resembles that for argon[29,30] and suggests that only lattice vibrations make significant contributions to the heat capacity in this temperature range. By extrapolating the points below $T^2 = 43\ K^2$ to intersect the $C_{p,m}/RT^3$ axis at $T^2 = 0$, we found $10^4 \cdot a/R = (3.60 \pm 0.60)\ K^{-3}$ or $10^4 \cdot a = (29.93 \pm 5.0)\ J \cdot K^{-1} \cdot mol^{-1}$, which yields from equation (5) $\Theta_0^C = (86.6 \pm 4.3)$ K. This may be compared with 93.3 K for argon,[29] (83.6 ± 5.9) K for $(NH_4)_2TeCl_6$,[7] 83.7 K for $(NH_4)_2PtCl_6$,[6] and 92.1 K for $(ND_4)_2PtCl_6$.[7]

Neutron-diffraction experiments have yet to be done on $(ND_4)_2TeCl_6$. However, our heat-capacity results described above, together with the n.q.r. and Raman findings reported in reference 11, support the presence of a rotative displacive transition around $T = 87$ K, similar to that confirmed in the undeuterated salt. For our $(ND_4)_2TeCl_6$, the continuous curve of heat capacity against temperature and low values of molar enthalpy: $\Delta_{trs}H^\circ_m = (19.22 \pm 0.04) \cdot R \cdot K$, and molar entropy: $\Delta_{trs}S^\circ_m = (0.234 \pm 0.006) \cdot R$, are consistent with a subtle change in orientation of the anions.

The λ-shaped transitions in the heat capacity of $(ND_4)_2TeCl_6$ at $T = 47.6$ K and $T = 31.4$ K occur within the temperature range where anomalies were found respectively in the ^{35}Cl n.q.r. and deuteron spin-lattice relaxation rates.[11] These anomalies are thought to be due to the change in the motion and orientation of the ND_4^+.[8,11] It is likely that crystallographic studies will confirm the presence of a phase III and phase IV above and below $T = 31.4$ K, respectively. For the likely structural change at $T = 47.6$ K, the low value of $\Delta_{trs}S^\circ_m = (0.247 \pm 0.006) \cdot R$ suggests a subtle change in orientation. However, at $T = 31.4$ K, the larger value of $\Delta_{trs}S^\circ_m = (0.861 \pm 0.007) \cdot R$ may be indicative of a more significant structural change. The crystal structure needs to be determined just above $T = 47.6$ K, between $T = 47.6$ K and $T = 31.4$ K, and below $T = 31.4$ K.

Note added in proof. The results of neutron-diffraction measurements just published by Kume *et al.* in *Europhysics Letters* **1991,** 16, 265 show structural changes from tetragonal below $T = 31$ K to monoclinic up to 48 K to rhombohedral up to 87 K to cubic above 87 K.

We thank Drs J. Pelzl, R. L. Armstrong, and B. M. Powell for making the sample available and Dr R. D. Heyding for determining its crystal structure just prior to loading. We also thank Mrs J. Hale for help with the calculations. Two of us (JEC, RDW) acknowledge the Department of National Defence (Canada) for financial support.

REFERENCES

1. Regelsberger, M.; Pelz, J. *Solid State Commun.* **1978,** 28, 783.
2. Morfee, R. G. S.; Staveley, L. A. K.; Walters, S. T.; Wigley, D. L. *J. Phys. Chem. Solids* **1960,** 13, 132.
3. Armstrong, R. L.; Mintz, D.; Powell, B. M.; Buyers, W. J. L. *Phys. Rev.* **1978,** B17, 1260.

4. Mintz, D.; Armstrong, R. L.; Powell, B. M.; Buyers, W. J. L. *Phys. Rev.* **1979,** B19, 448.
5. Callanan, J. E.; Weir, R. D.; Westrum, E. F., Jr. *J. Chem. Thermodynamics* to be published.
6. Weir, R. D.; Westrum, E. F., Jr. *J. Chem. Thermodynamics* **1990,** 22, 1097.
7. Weir, R. D.; Westrum, E. F., Jr. *J. Chem. Thermodynamics* **1991,** 23, 653.
8. Kawald, W.; Müller, S.; Pelzl, J.; Dimitropoulos, C. *Solid State Commun.* **1988,** 67, 239.
9. Dimitropoulos, C.; Pelzl, J. *Z. Naturforsch.* **1989,** A44, 109.
10. Furukawa, Y.; Nakamura, D. *Ber. Bunsenges. Phys. Chem.* **1989,** 93, 13.
11. Dimitropoulos, C.; Pelzl, J.; Borsa, F. *Phys. Rev.* **1990,** 41, 3914.
12. Callanan, J. E.; Weir, R. D.; Westrum, E. F., Jr. *J. Chem. Thermodynamics* **1992,** 24, 567.
13. Wyckoff, R. W. G. *Crystal Structures, Vol. 3.* Interscience: New York. **1965,** p. 342.
14. Engel, G. *Central. Mineral. Geol.* **1934,** 1934A, 285.
15. Engel, G. *Z. Kristallogr.* **1935,** 90A, 341.
16. Westrum, E. F., Jr.; Furukawa, G. T.; McCullough, J. P. *Experimental Thermodynamics, Vol. 1.* McCullough, J. P.; Scott, D. W.: editors. Butterworths: London. **1968,** p. 133.
17. Stimson, H. F. *J. Res. Natl. Bur. Stand. (U.S.)* **1961,** 65A, 139.
18. McCrackin, F. L.; Chang, S. S. *Rev. Sci. Instrum.* **1975,** 46, 550.
19. Chirico, R. D.; Westrum, E. F., Jr. *J. Chem. Thermodynamics* **1980,** 12, 311.
20. Goldberg, R. N.; Weir, R. D. *Pure Appl. Chem.* in the press.
21. Bedford, R. E.; Durieux, M.; Muijlwijk, R.; Barber, C. R. *Metrologia* **1969,** 5, 47.
22. Westrum, E. F., Jr. *Proceedings NATO Advanced Study Institute on Thermochemistry, Viana do Castello, Portugal.* Ribeiro da Silva, M. A. V.: editor. Reidel: New York. **1984,** p. 745.
23. Andrews, J. T. S.; Norton, P. A.; Westrum, E. F., Jr. *J. Chem. Thermodynamics* **1978,** 10, 949.
24. *Pure Appl. Chem.* **1986,** 58, 1678.
25. Staveley, L. A. K.; Grey, N. R.; Layzell, M. J. *Z. Naturforsch.* **1963,** 18A, 148.
26. Morphee, R. G. S.; Staveley, L. A. K. *Nature* **1957,** 180, 1246.
27. Miller, G. R.; Gutowsky, H. S. *J. Chem. Phys.* **1963,** 39, 1983.
28. Barron, T. H. K.; Berg, W. T.; Morrison, J. A. *Proc. Roy. Soc. London* **1957,** A242, 478.
29. Beaumont, R. H.; Chihara, H.; Morrison, J. A. *Proc. Roy. Soc. London* **1961,** 78, 1462.
30. Finegold, L.; Phillips, N. E. *Phys. Rev.* **1969,** 177, 1383.